

Model-based seafloor characterization employing multi-beam angular backscatter data – a comparative study with dual-frequency single beam.

Haris K¹, Bishwajit Chakraborty^{1,*}, Chanchal De², Prabhudesai R.G¹, and William Fernandes¹

¹National Institute of Oceanography, Council of Scientific and Industrial Research, Dona Paula, Goa: 403 004, India

²G-FAST, P1-Metcalf House, Delhi-110054, India

* Correspondence to: Geological Oceanography division, National Institute of Oceanography, Dona Paula, Goa: 403 004

Electronic mail: bishwajit@nio.org (B. Chakraborty)

Abstract:

Sediment geoacoustic inversion results are estimated employing a multi-beam (MB) echo-sounding system operable at 95 kHz. In order to characterize the western continental shelf of India (off Goa) seafloor, MB backscatter signals were acquired along with grab sediment samples. The substrate type and roughness of the site were estimated using the composite roughness scattering model with the measured backscatter values. The seafloor parameters, namely mean grain size (M_{ϕ}); roughness spectrum strength (w_2) and exponent (ν_2); and sediment volume parameter (σ_2), for coarse and fine grain sediments are estimated by employing the MB system. These parameters have also been estimated at two other frequencies (33 and 210 kHz), and are compared to the ground truth data to provide sufficient support in validating the model results and increasing the understanding of the shelf seafloor processes. Distinct interclass separations between the sediment provinces are evident from the estimated mean grain size M_{ϕ} and water-sediment interface roughness w_2 . The seafloor parameters for coarse and fine grain sediments derived from the 95 kHz MB data are consistent with the sediment sample data as well as with the inversion results obtained using backscatter data at 33 and 210 kHz from the same locations.

I. INTRODUCTION

The employment of remote acoustic techniques for seafloor characterization involving high-frequency echo-sounding systems¹ such as multi-beam (MB) and single-beam (SB) operable within 10-300 kHz is well established. Numerical approaches like “inversion modeling” provide upper-layer seafloor roughness parameters, namely the sediment mean grain size (M_{ϕ}); spectral parameters at the water-seafloor interface (r_2, w_2); and sediment volume parameter (σ_2).² The composite roughness model using the shape of the angular backscatter function developed by Jackson *et al.*,³ has been extensively applied to this approach.⁴⁻⁶ In this work, characterization of seafloor sediments is achieved by employing a MB system (Simrad EM 1002) operable at 95 kHz. Here, the seafloor parameters are estimated by applying the composite-roughness theory to angular backscatter strength data collected from coarse- and fine- grained seafloor sediments at 12 locations on the western continental shelf of India (off Goa) and these parameters are used for inversion modeling.

Moving beyond techniques that employ the angular backscatter strength, Pouliquen and Lurton⁷ initiated a modeling method using echo envelope shapes. Sternlicht and de Moustier⁸⁻¹⁰ also presented an extensive time-dependent echo envelope model, which is extended for seafloor characterization¹¹ using a normal-incidence SB system. Moreover, the use of multiple acoustic frequencies increases the ability to characterize the seafloor sediment because the roughness spectrum and the volume backscattering strengths cause frequency dependence that can be exploited in multi-frequency seafloor classification.¹² The aim of this work is to characterize seafloor sediment with three frequencies employing MB and dual-frequency SB systems operable at 95 kHz and 33 and 210 kHz, respectively. The estimated seafloor parameters for coarse and fine-grain sediments from the 95 kHz MB are compared with the inversion results previously obtained with the SB echo envelope data from the 33 and 210 kHz at the same locations.¹¹ The sediment mean grain sizes of a Van-Veen grab sampler from the shallow depth region off Goa are used as a ground truth for the validation of model results.

The work is organized as followed. Section II titled “materials and methods” covers the MB backscatter and the sediment sample data acquisition from the shelf region. Section III discusses the simulated annealing with the downhill simplex method for estimating roughness parameters using angular backscatter model-data matching. Presented in section IV is the comprehensive analyses of the estimated roughness parameters and their comparisons with those estimated using the SB echo envelope output. Finally, the conclusions are provided in section V.

II. MATERIALS AND METHODS

A. Backscatter data acquisition and sediment sampling

MB seafloor backscatter data was acquired over substrates ranging from clayey silt to sand in the central part of the western continental shelf of India [Fig. 1(a)]. The 95 kHz MB having 111 pre-formed beams data were acquired during two cruises using the EM1002 echo-sounding system installed onboard CRV *Sagar Sukti* (cruises: SASU-108 and 134).^{13,14} Besides calculating the angular backscatter strengths using the MB system, the modeled results¹¹ of the 33 and 210 kHz echo waveforms are also analyzed in order to compare the results.

Figure 1(a) shows the 12 spot locations where the backscatter data (MB and SB) and sediment sample data were collected. The data was acquired along the two tracks located towards the northern as well as southern part of the Mormugao port (off Goa). The seafloor depth for the present study locations generally varies between 29-109m. Sediment samples were analyzed for textural studies using a Van-Veen grab following standard protocol. The acquired sediment samples were put through a 62 μm sieve to separate the sand from the mud fraction employing wet sieving. The size distribution (<62 μm) of the mud fraction was measured with a Malvern laser particle size analyzer (MASTERSIZER 2000). Since it was very difficult to maintain uniform suspension of sandy material within the laser particle analyzer, the size distribution of the sand fraction was determined using standard dry sieving method.¹⁵ The shelf sediments also frequently contain shelly material, which have to be sieved prior to the measurement by laser diffraction. The percentage distribution of sediment compositions (based on Shepard's classification¹⁶) shows the presence of four seafloor sediment types: clayey-silt, silt, silty-sand and sand (Table 1). The mean grain size $M_{\phi} = -\log_2 U_{\phi}$ (where U_{ϕ} is the mean grain size diameter of the sediment samples) was then calculated for each of the sediment sample locations.

B. Multi-beam (MB) data processing

1. Corrections made within the sonar

During the time of data acquisition, the Simrad EM 1002 system primarily measures the time average of the received backscattered signal envelope (EL) in each of its 111 beams. The received signal envelopes are corrected for time variable gain (TVG), predicted beam patterns, and the insonified area. This data then gets recorded in a packet format called "datagram" and is stored for every ping as estimates of the seafloor's backscatter strength.¹⁷ However, such data recorded by the system is not directly usable for a correct estimation of the backscattering strength angular dependence. Hence, post

processing is essential to be carried out for the removal of Lambert's law, corrections for actual bottom slope and the insonified area.¹⁷ However, if the sonar is not routinely calibrated the backscatter values obtained after the post processing are probably not accurate (i.e., the reference level is effectively arbitrary), but they are nevertheless likely to be sufficiently reliable in a relative sense to record differences between sediment types. Consequently, even after post processing, prior to model-data comparison, there was a lack of absolute calibration and a depth-dependent offset (scaling parameter in dB) was required to add to each of the processed data sets.

The corrections applied by the echo-sounder to the echo level (EL) of the signal backscattered may be derived from the sonar equation:

$$EL = SL - 2TL + TS \quad (1)$$

where SL is the multi-beam echo sounder source level, $2TL$ is the two-way transmission loss, and TS is the target strength which includes the local backscattering strength, the insonified area and Lambert's law to normalize the acoustic image of the seafloor.¹⁸

In normal operation mode, the MB system applies a time variable gain (TVG) to the received signals in order to compensate for beam spreading and absorption losses. The purpose of TVG is to maintain a constant sensitivity for the observation of a given target at any range. The TVG must be predicted before reception (based on previous pings), and must be planned so that the average signal level in the receiver is at an optimum level in order to avoid saturation or clipping of the echo envelope. An additional reason for running such TVG is that it will flatten the beam sample amplitudes. This is beneficial for bottom detection, but also important for display of the seabed image.¹⁷

2. Post processing of the sonar output

In order to obtain a correct angular backscattering strength, the PROBASI-II (PROcessing BACKscatter SIGNAL) algorithm¹⁹ was employed to raw backscatter data to make necessary corrections related to position, heading, bathymetry slope, seafloor insonified area, and also Lambert's law corrections. The raw backscatter data mentioned here corresponds to echo level (EL) in Eq. (1), i.e., it features the various compensations by the sonar's own processing. In order to apply the above mentioned corrections during post processing, a batch file was created consisting of EM1002 echo-sounder's raw data. The program first read this batch file and extracted specific data such as backscatter strength, bathymetry, heading, position, and beam angle required during the processing of backscatter intensities.

a. Heading and position correction

Initially, during the time of data acquisition, the data is corrected for motion. However, when the ship turns to change the survey track it is found that the data is not compensated properly for heading, likely due to latency problem. Hence, the developed algorithm applies heading corrections when required. By comparing initial and next heading data the required heading offsets are calculated. Besides heading corrections, the accuracy of used DGPS's differs, likely due to the unavailability of the shore station or GPS satellites, and at those times the system records wrong positions. Consequently, the backscatter strengths are recorded with the wrong position indicating data from unknown locations. Therefore, such a positional jump needs to be corrected before further analysis. In order to avoid such problems, the heading corrected data is monitored for any positional deviations and if necessary these are corrected using previous and next ping data.

b. Bathymetry slope and seafloor insonified area correction

Bathymetry slope has a significant effect on the backscatter strengths. Since the seabed slope varies across and along the swath, the beam incidence angles will also be changing. This will cause a shift in the positioning of the beams on the seabed. Such a shift will not be taken care of by the system since it assumes a flat seafloor. Accordingly, there will be variations in the backscatter strength, and these slope corrections were made during the processing of the raw backscatter strengths. During the time of data acquisition, the insonified areas incorporated in Eq. (1) are corrected with the simplifying assumptions of a flat seafloor. A revision of this area is needed if the bottom is not really flat. The updated insonified area on the seabed is then corrected by following the formula given in Ref. 17.

c. Lambert's law removal and corrected angular backscatter data

Finally, after giving the appropriate corrections for position, heading, bathymetry slope, and insonified area, the effect of Lambert's law was removed from the measured level given by the echosounder. The Lambert's law correction was introduced for homogenizing the sonar image, and it is not relevant for our purpose so it had to be eliminated. For inverse modeling, the processed MB angular backscatter data (in decibels) for 20 consecutive pings, varying between the incidence angles of -65° to $+65^{\circ}$ were binned in equal angular bins of 1° intervals. The data was then averaged over the available number of samples within each bin. Assuming that the angular backscatter function is symmetric about the normal incidence angle, this function was folded about the normal incidence angle, and represented from 0° to 65° only [Fig. 1 (d)].³⁻⁶

d. Backscatter image data processing

Moving beyond techniques that employ the processing of MB angular backscatter data for inversion modeling, the application of the PROBASI-II algorithm¹⁹ was further extended for backscatter image data generation. The PROBASI-II algorithm basically involves 4 modules, in which module 1 is used for correcting angular backscatter strengths to carry out inversion modeling. Besides the processing carried out in module 1, additional modules 2, 3, and 4 are employed for image data generation. Module 2 and 3 in the PROBASI- II algorithm comprised of: normalization of backscatter strengths to the 10⁰ incidence angle, angle wise averaging of backscatter strengths, and removal of beam pattern effects in two steps as coarse and fine methods to eliminate maximum residuals or spikes in the backscatter image data. Finally, in module 4, the noise was removed with the combination of low and high pass filters. The representative raw and processed images for locations 8 and 9 of this study area are also presented [Fig. 1 (b&c)] for improved perception of the seafloor.

III. MODEL-DATA COMPARISON

A. Estimation of scaling parameter to calibrate the data

Even after following the pre and post processing steps discussed in the above section, prior to model-data comparison, there was a lack of absolute calibration and a depth-dependent offset (scaling parameter in dB) should be corrected to each of the processed data sets. In order to estimate the scaling parameter (calibration offset) the backscattering strength *versus* grazing angle functions were derived from the APL-UW (1994) seabed scattering model² using sediment mean grain size M_{ϕ} (the ground truth sediment information) for a set of related geoacoustics parameters. The seabed angular scattering model² for MB combines the most dominant dimensionless scattering mechanism of the surface roughness coefficient $S_s(\theta_g)$ and volume scattering coefficient $S_v(\theta_g)$ as a superposition of the incoherent scatter to estimate the total seabed backscattering strength $BS_{model}(\theta_g)$ as:

$$BS_{model}(\theta_g) = 10 \log_{10}[S_s(\theta_g) + S_v(\theta_g)] \text{ dB} \quad (2)$$

where θ_g is the grazing angle (90⁰-incidence angle). There is a difference between the APL-UW model prediction and the processed MB data for fine and coarse sediment regions [Fig 2 (a)]. These differences may be due to instrument calibration or model accuracy.²⁰⁻²² As discussed in the previous section, the sonar TVG is not accurate. Consequently, even after post processing, the measured backscatter levels must be treated as relative in order to make proper comparisons with scattering models.^{20, 22}

In order to maximize the fitting process and to match the relative backscatter values of the model and measured data, the error-to-signal (E/S) ratio is used as a merit function with the goal of minimizing this value. The E/S is expressed as $E/S = \frac{\sum_{\theta_g=11}^{\theta_g=114} (BS_{data}[\theta_g] - BS_{model}[\theta_g])^2}{\sum_{\theta_g=11}^{\theta_g=114} BS_{data}[\theta_g]}$, where the terms $BS_{data}[\theta_g]$ and $BS_{model}[\theta_g]$ represent the data and model predicted backscatter values. This method provides a numerical evaluation which is independent of scale and backscatter angular range, and is convenient for comparing the model and data.¹¹ The corresponding scaling parameter in dB (difference between model and data), which minimizes the E/S ratio is used as the representative scaling factor for that particular data. The scaling parameters at 12 locations from the study area having coarse and fine sediments are estimated. The scatter diagram between the estimated scaling parameters and water depths of the spot locations shows a correlation coefficient of 0.85 [Fig. 2(b)]. Finally, for inverse modeling, the processed backscatter data for all grazing angles was adjusted by a scaling parameter in accordance with the water depth of the spot locations following the linear fitted line obtained from the scatter diagram.

B. Two-stage parametric optimization

The estimation of seafloor geoacoustics parameters is complicated by the large number of good fits existing in the multidimensional search space where it is possible to find convincing model-data fits which do not necessarily represent correct solutions. This is why, we parsed the problem into a two stage parametric optimization¹⁰ by constraining the search space. There are several options to quantify the matching result between the data and model. Here, as discussed above, we have chosen as the cost-function the error to signal ratio (E/S) with the goal of minimizing the values. In this framework, a low value of E/S signifies a “good” model to data match. Sternlicht and de Moustier¹⁰ used simulated annealing with the downhill simplex method to estimate the parameters M_{φ} , w_2 , and σ_v by echo envelope matching using a 3D global search method. In the present study, we used a 4D global search technique including γ_2 and replaced the sediment volume scattering coefficient (σ_v) with the sediment volume scattering parameter (σ_2).¹¹ The first stage of the model-data matching procedure employs a 1D search to estimate the general values of the sediment mean grain size (M_{φ}). The output of the 1D search process provides the starting M_{φ} value for the second stage 4D global search method to estimate the refined mean grain size (M_{φ}); the roughness spectral exponent (γ_2) and strength (w_2); and the sediment

volume parameter (σ_2). Here, the above mentioned technique was employed to estimate seafloor parameters using MB system data.

IV. RESULTS AND DISCUSSION

In this section, we compare the estimated seafloor parameters of the angular backscatter MB data with the echo envelope data of normal incidence SB systems using the composite roughness scattering model for the 12 study locations on the continental shelf. This study also provides a comparison between the estimated seafloor parameters at three frequencies to assess the modeling performance and bottom characterization potentialities. The end results (given in Table 2) are statistically analyzed and compared to the ground truth data, as well as information available in published literature. Figure 3 shows the model-data fit for three geologically distinct sediment provinces. For simplicity, in the following text silty-sand and sand sediments will be referred to as coarse sediments (with estimated $M_\phi < 4\phi$); and clayey-silt and silt sediments will be referred to as fine sediments (with estimated $M_\phi > 4\phi$).

A. Estimated mean grain size (M_ϕ) parameter

The peak amplitudes of echo envelopes primarily depend on the impedance contrast between the water and seafloor sediments. In surficial sediments, the impedance contrast is often correlated with the mean grain size of sediments.⁹ The estimated mean values of M_ϕ of surficial sediments obtained with echo envelope inversions from the study locations are found to correlate well with the measurements (95% of confidence limit).¹¹ Hence, in the present study the estimated values of M_ϕ obtained from the inversions of angular backscatter strength of MB also should correlate with the measurements (based on sediment ground truth) and / or information from De and Chakraborty¹¹ for the same locations. In view of this, the estimated M_ϕ values for three different acoustic frequencies are presented as a function of the measured M_ϕ values [Fig. 4]. On the whole, the estimated M_ϕ values agree well with the measured sediment data, having correlation coefficients of 0.97, 0.98, and 0.96 for 33, 95, and 210 kHz, respectively.

The linear regression analysis carried out for the inversion results of normal-incidence SB¹¹ data from the study locations indicates that the least-squares line obtained from the best fit of 33-kHz data gives the best estimation of M_ϕ . In order to validate the presently estimated M_ϕ using MB data, correlation analyses have been carried out between model-estimated M_ϕ parameters of SB and MB

results. Excellent correlations of 0.97, 0.97 and 0.98 have been obtained between model-estimated M_{ϕ} parameters from 33 and 210 kHz, 33 and 95 kHz, and 95 and 210 kHz respectively. Therefore, compared to the SB results, the model-data match for MB results as a function of grazing angle exhibit equivalent consistency in the estimation of M_{ϕ} for seafloor characterization.

On the whole, the estimated values of the mean grain size (M_{ϕ}) agree with the ground-truth measurements. However, minor fluctuations in the estimated M_{ϕ} parameters for 33, 95, and 210 kHz, with respect to ground truth data are also observed. The backscatter strength from the sea floor is primarily controlled by the acoustic frequency, the acoustic impedance contrast between water and sediment, the contributions from seafloor interface roughness, as well as sediment volume inhomogeneity. In soft sediments, the acoustic energy (both high and low frequency signal) penetrates into the sediment and is likely to be scattered from buried inhomogeneities such as coarse sand particles and mollusk shells.¹¹ These can lead to local deviation of impedance contrast from the generic values (values correlated with M_{ϕ}) employed by the model-data matching techniques.⁹ As the estimated parameter is especially sensitive to changes in the acoustic impedance (the product of density and sound speed in the sediment), the variation of density within the sediment may contribute to disagreements between the model-data matches and ground truth.

B. Estimated seafloor roughness parameters (γ_2 and w_2)

In order to understand the relationship between the backscatter and relief spectral parameters, we have estimated the seafloor roughness (γ_2 and w_2) parameters at 95 kHz. Thereafter, an analysis is carried out using the estimated seafloor roughness parameters of MB and dual-frequency SB data¹¹ [Figs. 5&6]. The scatter diagram between measured values of M_{ϕ} and estimated γ_2 [Fig. 5] show that, for coarse sediments, the values of γ_2 are confined within the limits of 3.10 to 3.25, 3.15 to 3.24, 3.10 to 3.20, respectively, for 33, 95, and 210 kHz. Whereas, for fine sediments, the estimated γ_2 values lie within the limits of 3.21 to 3.32, 3.21 to 3.27, 3.22 to 3.34, for 33, 95, and 210 kHz respectively. Moreover, for coarse sediments, the overall average estimates of γ_2 are found to be 3.18 ± 0.061 , 3.19 ± 0.032 , and 3.14 ± 0.047 , respectively, for 33, 95, and 210 kHz. But for fine sediments, the overall average estimates of γ_2 are 3.23 ± 0.085 , 3.22 ± 0.020 , and 3.28 ± 0.043 , respectively, for 33, 95, and 210

kHz. It is observed that higher values of γ_2 are associated with fine sediments, and in contrast lower values of γ_2 are associated with coarse sediments.

The seafloor roughness power spectrum estimated from the relative height measurements is a characterization of the variance of the size and periodicity of the seafloor height fluctuations as a function of the spatial frequency.²³ The roughness power spectrum is often parameterized using a power law by the slope and intercept of the linear regression line through the points of the periodogram estimate in *log-log* space. In fact, the parameters γ_2 and w_2 used in the scattering model of Jackson *et al.*,³ are actually the slope and intercept, respectively, of the 2D roughness power spectrum, which are estimated from the 1D power-law values. A wide range of these 2D roughness power spectrum parameters are thus available in literature,²³⁻²⁶ and indicate that the majority of the values of the 2D spectral exponent are confined within the limits of 2.90 to 3.30 for coarse sediments and 3.20 to 3.50 for fine sediments. In the present study the estimated γ_2 values are found to be in agreement with the published data, but have a narrower range of values.

Several field experiments^{25, 27} revealed that the majority of the measured values of 2D spectral strength (w_2) are greater than 0.002 cm^4 for coarse sediments, and are restricted to values around 0.003 cm^4 for fine sediments.⁹ The scatter diagram between the measured values of M_{ϕ} and estimated w_2 [Fig. 6] revealed that the values of w_2 are less than 0.001 cm^4 for fine sediments and are confined within 0.002 to 0.005 cm^4 for coarse sediments from all the three inversion results. Moreover, for coarse sediments, the overall average estimates of w_2 are found to be 0.0037 ± 0.00028 , 0.0037 ± 0.00032 and 0.0040 ± 0.00074 , respectively, for 33, 95, and 210 kHz. But for fine sediments, the overall average estimates of w_2 are 0.00057 ± 0.000052 , 0.00052 ± 0.000043 , and 0.00060 ± 0.000054 , respectively, for 33, 95, and 210 kHz. On the whole, the values of w_2 at the three frequencies are found to be in good agreement with the published information. It is observed that the estimated values of w_2 are well clustered, having less fluctuations for fine sediments than for coarse sediments at all acoustic frequencies [Fig. 6]. Moreover, it is also observed that higher values of w_2 and lower values of γ_2 are associated with coarse sediments, while lower values of w_2 and higher values of γ_2 characteristics are found for fine sediments.

Briggs *et al.*,²³ and Jackson and Richardson¹ reported that the values of w_2 and γ_2 appeared to be weakly clustered according to sediment type with separate trends for coarse and fine sediments. In the present analysis similar clustering of roughness parameters for fine-and coarse-grained sediments are also evident [Fig. 5 &6]. Briggs²⁴ also reported that the parameters derived from a roughness power spectrum vary with the sediment type, such that the roughness spectra characteristic of coarse sediments have a less-steep decay (i.e., lower value of γ_2) in the power-law relationship. One of the possibilities for a power spectrum to have a less-steep decay (i.e., less-steep slope of the regression line) is that the intercept energy of the spectrum at a unit spatial frequency (1cm) is high (i.e., higher value of w_2).⁹ Thus, coarse sediments are associated with higher values of w_2 and lower values of γ_2 . Conversely, fine sediments are associated with comparatively lower values of w_2 and higher values of γ_2 . These aspects are also evident in the present analysis [Fig. 5&6].

C. Estimated sediment volume parameter (σ_2)

The sediment volume parameter (σ_2) controls the level of the tail portion of the echo envelope. Generally, σ_2 values are functions of the seafloor sediment type (fine or coarse) and seafloor inhomogeneities.³ Jackson and Briggs²⁸ demonstrated dominant sediment volume backscatter for finer sediment, and Jackson *et al.*,³ considered it as a free parameter with a maximum value up to 0.004 for soft sediment. However, Stewart and Chotiros²⁹ have experimentally shown that the limit imposed for soft sediment is low, and the sediment volume scattering coefficient is usually much higher than the predicted value. Nevertheless, it is preferable to use the estimated σ_2 as a fitting parameter for different locations as a means to understand the seafloor processes. The sensitivity analysis of σ_2 on the echo envelope shape indicates that as σ_2 increases the contribution of sub-bottom scattering becomes prominent near the tail portion of the echo envelope. The peak amplitude of the total echo envelope, however, changes marginally with an increase in the value of σ_2 . According to a recent study using SB systems in this area,¹¹ the low values of σ_2 (<0.004) produced high values of E/S ratio in the model-data matching process. By increasing the value of this free parameter σ_2 (>0.004), the level of the predicted backscatter strength was increased to that of the observed data with low values of E/S ratio. Also, the estimated σ_2 was found to be the most difficult to interpret, as it is considered to be a fitted parameter that varies with location. Hence, in the absence of detailed information on sediment volume scattering

for modeling, based on SB results,¹¹ the initial volume parameter for MB data modeling is assigned as 0.004 for all sediment types.

For coarse sediments, the overall average estimates of σ_2 are found to be 0.0039 ± 0.00059 , 0.0034 ± 0.00063 , and 0.0031 ± 0.00048 , respectively, for 33, 95, and 210 kHz. But for fine sediments, the overall average estimates of σ_2 are 0.0047 ± 0.00056 , 0.0045 ± 0.00021 , and 0.0043 ± 0.00026 , respectively, for 33, 95, and 210 kHz. These values of σ_2 are necessary to provide reasonable model-data fits at the three acoustic frequencies (Fig. 7). Jackson and Briggs²⁸ reported that the volume scattering will be dominant for soft sediments. The experiment conducted by them revealed that the predicted model matches well with the observed data, if relatively high values of σ_2 (0.004 to 0.006) are used for soft sediments. Thus, large values of σ_2 may be required to get the best model-data fit for soft sediments. In the present study, for fine sediments, the average estimates of σ_2 are found to be higher when compared to coarse sediment regions for all the three acoustic frequencies. In addition to this, no definite relationship between the estimated mean values of σ_2 and the mean grain size is found in the study area.¹¹ The assessment on the correctness of these values is difficult in the absence of ground-truth data and further study in conjunction with the same is required for a better conclusion.

V. CONCLUSIONS

The seafloor parameters estimated using the Simrad EM1002 MB (angular backscatter) at 95 kHz, and RESON-NS 420 SB (echo envelope shape) at dual frequencies (33, 210 kHz) are compared employing the composite roughness scattering model³ to determine the mean grain size (M_g) and roughness parameters (γ_2 and w_2) from the western continental shelf of India. The sediment textural properties were collected using a grab for ground truth data. The set of estimated geoaoustics parameters provides useful information that can be utilized for seafloor characterization. In the absence of geo-referenced measured roughness data, the analysis of the estimated geoaoustics parameters for different combinations of sediment type and frequency suggests that the 95 kHz MB results are suitable for sediment characterization. The objective of this work was to establish a link between angular backscatter inversion results from MB data with results from normal-incidence SB data.¹¹ There is excellent correlation ($r=0.97$, 0.97 and 0.98) between model-estimated M_g parameters from 33 and 210 kHz, 33 and 95 kHz, and 95 and 210 kHz data, respectively. The values of mean grain size estimated from the 33 and 95 kHz inversions provide relatively improved results with respect to the ground-truth

data over the 210 kHz inversion results. In the absence of the measured roughness data, the estimated values of roughness spectrum parameters (γ_2 and w_2) are compared with reference to the available published information. These estimated values of γ_2 and w_2 from the three inversion results are found to be consistent with the published data, however, minor variations in the estimated roughness parameters between the 33- and 95-kHz data with respect to the 210 kHz data are also known to occur.¹¹ Williams *et al.*,³⁰ revealed that the physics behind the backscattering mechanism appeared to be changing in the critical frequency region of 150 to 300 kHz. Recently, Williams *et al.*,³¹ concluded that at 200 kHz or higher frequencies, a new scattering mechanism comes into play for the backscatter data obtained from both the SAX99 and SAX04 experiments. At high frequencies (150 kHz to 2 MHz), a significant difference in scattering strength from the surrounding medium and the embedded coarse material in controlled laboratory experiments is also observed.³² Moreover, it has been reported that at higher frequencies (> 200 kHz), even a small portion of embedded shell fragments could significantly change the seafloor scattering characteristics. Such scattering mechanisms in the critical region of the frequency range from 150-200 kHz may possibly be responsible for the minor fluctuations in the estimated roughness parameters between the 33- and 95-kHz data with respect to the 210 kHz data. Our present work indicates that the predicted seafloor parameters from the 95 kHz inversions more closely match the inversion results from 33 kHz data than the results from 210 kHz data.

ACKNOWLEDGEMENTS

We are thankful to Dr. S.R. Shetye, Director, National Institute of Oceanography, for his permission to publish this work. Support under the Ocean Acoustics Program of the National Institute of Ocean Technology (NIOT) is gratefully acknowledged. We are also thankful to Dr. J.N. Pattan and Dr. P. Kessarker for the sediment data. Help from Dr. G. Latha, Principal Investigator, Mr. Ryan Rundle, Florida Atlantic University, USA, and encouragement from Dr. M. Atmanand, Director, NIOT is also duly acknowledged. K. Haris expresses thanks to Council of Scientific and Industrial Research (CSIR), India for his fellowship. The authors are grateful to the reviewers for suggestions to improve the clarity of this manuscript.

REFERENCES

- ¹D. R. Jackson and M. D. Richardson, “*High-Frequency Seafloor Acoustics*,” New York: Springer-Verlag, Chap. 13, pp. 331-376, 2007.
- ²Applied Physics Laboratory. High Frequency Ocean Environmental Acoustic Models Handbook. Technical Report, APL-UW TR 9407, AEAS 9501 University of Washington, Chap. 4, 1994.
- ³D. R. Jackson, D. P. Winebrenner, and A. Ishimaru, “Application of the composite roughness model to high-frequency bottom backscattering,” *J. Acoust. Soc. Am.* **79**, 1410-1422 (1986).
- ⁴C. de Moustier and D. Alexandrou, “Angular dependence of 12-kHz seafloor acoustic backscatter,” *J. Acoust. Soc. Am.* **90**(1), 522-531 (1991).
- ⁵H. Matsumoto, R. P. Dziak, and C.G. Fox, “Estimation of seafloor microtopographic roughness through modeling of acoustic backscatter data recorded by multi-beam systems,” *J. Acoust. Soc. Am.* **94**(5), 2776-2787 (1993).
- ⁶B. Chakraborty, V. Kodagali, and J. Baracho, “Seafloor classification using multibeam echo sounder angular backscatter data: a real time approach employing hybrid neural network architecture,” *IEEE J. Oceanic Eng.* **28**, 121-128 (2003).
- ⁷E. Pouliquen and X. Lurton, “Sea-bed identification using echo-sounder signals,” in European conference on underwater acoustics, edited by M. Weydert, Elsevier Applied Science, London, pp. 535-538, 1992.
- ⁸D. D. Sternlicht and C. P. de Moustier, “Temporal modeling of high frequency (30-100 kHz) acoustic seafloor backscatter: shallow water results,” in Proceedings of High Frequency Acoustics in Shallow Water, N. G. Pace, E. Poliquen, O. Bergen, and A. P. Lyons (Eds.), NATO SACLANT Undersea Res. Ctr., La Spezia, Italy, pp. 509-516, 1997.
- ⁹D. D. Sternlicht and C. P. de Moustier, “Time dependent seafloor acoustic backscatter (10-100 kHz),” *J. Acoust. Soc. Am.* **114**, 2709-2725 (2003).
- ¹⁰D. D. Sternlicht and C. P. de Moustier, “Remote sensing of sediment characteristics by optimized echo-envelope matching,” *J. Acoust. Soc. Am.* **114**, 2727-2743 (2003).
- ¹¹C. De and B. Chakraborty, “Model based acoustic remote sensing of seafloor characteristics,” *IEEE Trans. Geosci. Rem. Sens.* May (2011) [DOI: 10.1109/TGRS.2011.2139218].
- ¹²P. A. van Walree, M. A. Ainslie, and D. G. Simons, “Mean grain size mapping with single-beam echo sounders,” *J. Acoust. Soc. Am.* **120**(5), 2555-2566 (2006).
- ¹³Anonymous, “Sagar Sukti cruise report SASU-108,” Cruise report, National Institute of Oceanography, Dona Paula, Goa, India.

- ¹⁴Anonymous, "Sagar Sukti cruise report SASU-134," Cruise report, National Institute of Oceanography, Dona Paula, Goa, India.
- ¹⁵R. L. Folk, "*Petrology of Sediment Rocks*," Hemphills Publishing Company, Austin, Texas, pp. 170-171, 1968.
- ¹⁶F. P. Shepard, "Nomenclature based on sand-silt-clay ratios," *J. Sedimentary Petrology* **24**, 151-158 (1954).
- ¹⁷E. Hammerstad, "EM Technical Note: Backscattering and Seabed Image Reflectivity," Horten, Norway: Kongsberg Maritime AS, p. 5, 2000.
- ¹⁸X. Lurton, S. Dugelay and J. M. Augustin, "Analysis of multibeam echo-sounder signals from the deep seafloor," in *Proc. of IEEE Oceans'94*, pp. 213-218, 1994.
- ¹⁹W.A. Fernandes and B. Chakraborty, "Multi-beam backscatter image data processing techniques employed to EM 1002 system," in *Proceedings of the International Symposium on Ocean Electronics*, Kochi, India, pp. 93-99, 2009.
- ²⁰C. de Moustier and H. Matsumoto, "Seafloor acoustic remote sensing with multibeam echo-sounders and bathymetric sidescan sonar systems," *Mar. Geophys. Res.* **15**, 27-42 (1993).
- ²¹R.P. Dziak, H. Matsumoto and C.G. Fox, "Estimation of Seafloor Roughness spectral parameters from multi-beam sonar acoustic backscatter data: Axial Seamount, Juan de Fuca Ridge," *Geophysical Research Letters* **20**(17), 1863-1866 (1993).
- ²²R.J. Kloser, J.D. Penrose and A.J. Butler, "Multi-beam backscatter measurements used to infer seabed habitats," *Continental Shelf Research* **30**, 1772-1782 (2010).
- ²³K. B. Briggs, A. P. Lyons, E. Pouliquen, L. A. Mayer, and M. D. Richardson, "Seafloor roughness, sediment grain size, and temporal stability," in *Proc. Inter. Conf. Underwater Acoust. Meas.: Technol. Results*, J. P. Papadakis and L. Bjørnø (Eds.), Proceedings of a conference held in Heraklion, Crete, pp. 337-344, July 2005.
- ²⁴K. B. Briggs, "Microtopographical roughness of shallow-water continental shelves," *IEEE J. Ocean. Eng.* **14**(4), 360-367 (1989).
- ²⁵S. Stanic, K. B. Briggs, P. Fleischer, W. B. Sawyer, and R. I. Ray, "High-frequency acoustic backscattering from a coarse shell ocean bottom," *J. Acoust. Soc. Am.* **85**(1), 125-136 (1989).
- ²⁶D. R. Jackson, K. B. Briggs, K. L. Williams, and M. D. Richardson, "Test of models for high-frequency seafloor backscatter," *IEEE J. Ocean. Eng.* **21**, 458-470 (1996).
- ²⁷D. R. Jackson, A.M. Baird, J.J. Crisp and P.A.G. Thomson, "High-frequency bottom backscattering measurements in shallow water," *J. Acoust. Soc. Am.* **80**, 1188-1199 (1986).

- ²⁸D. R. Jackson and K. B. Briggs, "High-frequency bottom backscattering: Roughness vs. sediment volume scattering," *J. Acoust. Soc. Am.* **92**, 962-977 (1992).
- ²⁹R. A. Stewart and N. P. Chotiros, "Estimation of sediment volume scattering cross section and absorption loss coefficient," *J. Acoust. Soc. Am.* **91**, 3242-3247 (1992).
- ³⁰K. L. Williams, D. R. Jackson, E. I. Thorsos, D. Tang, and K. B. Briggs, "Acoustic backscattering experiments in a well characterized sand sediments: Data/model comparisons using sediment fluid and Biot models," *IEEE J. Ocean. Eng.* **27**, 376-387 (2002).
- ³¹K. L. Williams, D. R. Jackson, D. Tang, K. B. Briggs, and E. I. Thorsos, "Acoustic backscattering from a sand and a sand/mud environment: Experiments and data/model comparisons," *IEEE J. Ocean. Eng.* **34**(4), 388-398 (2009).
- ³²A. N. Ivakin, and J.-P. Sessarego, "High frequency broad band scattering from water-saturated granular sediments: Scaling effects," *J. Acoust. Soc. Am.* **122**(5), EL165-EL171 (2007).

TABLE I. Summary of the ground-truth data with the percentage composition of each sediment type.

Stn. No.	Sand (%)	Silt (%)	Clay (%)	Laboratory Measured M_{ϕ} (phi)	Sediment Type	Water Depth (m)
1	0.78	70.95	28.27	6.66	Clayey-silt	29
2	0.54	75.86	23.60	6.42	Silt	39
3	0.64	75.91	23.45	6.50	Silt	47
4	57.42	32.30	10.28	4.02	Silty-sand	54
5	0.13	70.66	29.21	6.79	Clayey-silt	42
6	0.92	79.05	20.03	6.20	Silt	53
7	80.90	14.24	4.86	2.42	Sand	60
8	89.05	8.65	2.30	1.16	Sand	66
9	70.31	24.45	5.24	2.40	Silty-sand	74
10	73.64	22.29	4.07	1.99	Silty-sand	87
11	54.58	38.52	6.90	3.32	Silty-sand	100
12	83.77	14.01	2.23	2.07	Sand	109

TABLE II. Summary of the seafloor parameters derived from three different acoustic frequencies 33 and 210 kHz (SB) and 95 kHz (MB) obtained through inversion modeling. The geoacoustic model input parameters are calculated from M_{ϕ} with the relationship described in Ref. 2.

Stn. No.	M_{ϕ} Measured (phi)	Estimated seafloor parameters at 33 kHz				Estimated seafloor parameters at 95 kHz				Error to signal ratio 95 kHz	Estimated seafloor parameters at 210 kHz			
		M_{ϕ} (phi)	γ_{ϕ}	w_{ϕ} (cm ⁴)	σ_{ϕ}	M_{ϕ} (phi)	γ_{ϕ}	w_{ϕ} (cm ⁴)	σ_{ϕ}		dB	M_{ϕ} (phi)	γ_{ϕ}	w_{ϕ} (cm ⁴)
1	6.66	6.96	3.32	0.000527	0.0037	6.67	3.26	0.000503	0.0045	-22	5.00	3.22	0.000524	0.0040
2	6.42	6.59	3.29	0.000561	0.0049	6.74	3.23	0.000512	0.0043	-26	4.75	3.27	0.000625	0.0040
3	6.50	6.29	3.10	0.000643	0.0049	6.53	3.21	0.000601	0.0044	-23	5.02	3.29	0.000670	0.0045
4	4.02	2.79	3.29	0.002370	0.0045	4.54	3.27	0.000917	0.0046	-24	3.08	3.12	0.001530	0.0041
5	6.79	6.71	3.21	0.000593	0.0050	6.75	3.21	0.000498	0.0048	-24	5.01	3.34	0.000582	0.0044
6	6.20	6.08	3.24	0.000516	0.0050	6.47	3.23	0.000510	0.0047	-26	4.21	3.28	0.000603	0.0045
7	2.42	1.97	3.12	0.00343	0.0046	1.99	3.15	0.00365	0.0041	-27	1.40	3.10	0.00401	0.0029
8	1.16	2.10	3.25	0.00365	0.0042	1.21	3.24	0.00375	0.0039	-23	1.31	3.14	0.00438	0.0040
9	2.40	2.37	3.24	0.00366	0.0043	2.10	3.21	0.00343	0.0038	-28	2.05	3.11	0.00255	0.0029
10	1.99	1.86	3.20	0.00419	0.0039	1.78	3.21	0.00428	0.0031	-29	1.10	3.10	0.00439	0.0027
11	3.32	2.33	3.19	0.00346	0.0038	2.17	3.18	0.00347	0.0034	-26	1.03	3.20	0.00452	0.0032
12	2.07	1.75	3.10	0.00388	0.0029	1.80	3.17	0.00397	0.0024	-24	1.51	3.20	0.00424	0.0028

FIGURE CAPTIONS

FIG. 1. Panel (a) shows the acoustic and sediment sample data acquisition locations and their sediment types: clayey-silt (cross), silt (square), silty-sand (closed-triangle) and sand (closed-diamond). The depth contours are in meters. The acoustic data was sampled with EM 1002 MB and RESON-NS 420 SB echo sounders along the two tracks. The panels (b) and (c) show typical applications of the PROBASI II algorithm for EM 1002 MB raw backscatter data. Panel (d) presents processed MB backscatter data at locations where inverse modeling was carried out.

FIG. 2. Panel (a) represents the model predictions of typical seabed types of silt (solid curve) and sand (dashed curve) using the geoacoustics model input parameters based on mean grain size M_ϕ of the ground truth data. The processed angular backscatter strengths for the same sediment types i.e., silt (dot-dashed curve) and sand (dot curve) are also presented. Note that clear separation between model predictions and substrate type backscatter is evident, and scaling parameters for 12 locations were obtained from the linear fit between the scaling parameters and water depths presented in panel (b).

FIG. 3. Panels (a), (b) and (c) represent the comparisons of the backscattering models and data for three geologically distinct sediment provinces: clayey-silt (location 1), silty-sand (location 10) and sand (location 8) respectively at 33-, 210-(SB) and 95-kHz (MB) frequencies. The solid curve represents the data, the dot-dashed curve for interface scattering, and the dashed curve shows the total, including sediment volume scattering (dot). The model-data comparison for the 95 kHz angular MB was done within the grazing angles 35° - 65° and the unfitted data (star) between 65° - 90° is also plotted.³

FIG.4. The scatter plot showing the relationship between the measured values of M_ϕ (phi) and the estimated values of M_ϕ (phi) for the three inversion cases.

FIG.5. The scatter diagram between the measured values of M_ϕ (phi) and the estimated spectral exponent γ_2 for the three inversion cases. The two blocks in the figure represent the boundaries of γ_2 for coarse and fine sediments.

FIG.6. The scatter diagram between the measured values of M_ϕ (phi) and the estimated spectral strength parameter w_2 (cm^4) for the three inversion cases. The two blocks in the figure represent the boundaries of w_2 for coarse and fine sediments.

FIG.7. The scatter diagram between the measured values of M_ϕ (phi) and the estimated sediment volume parameter σ_2 for the three inversion cases.

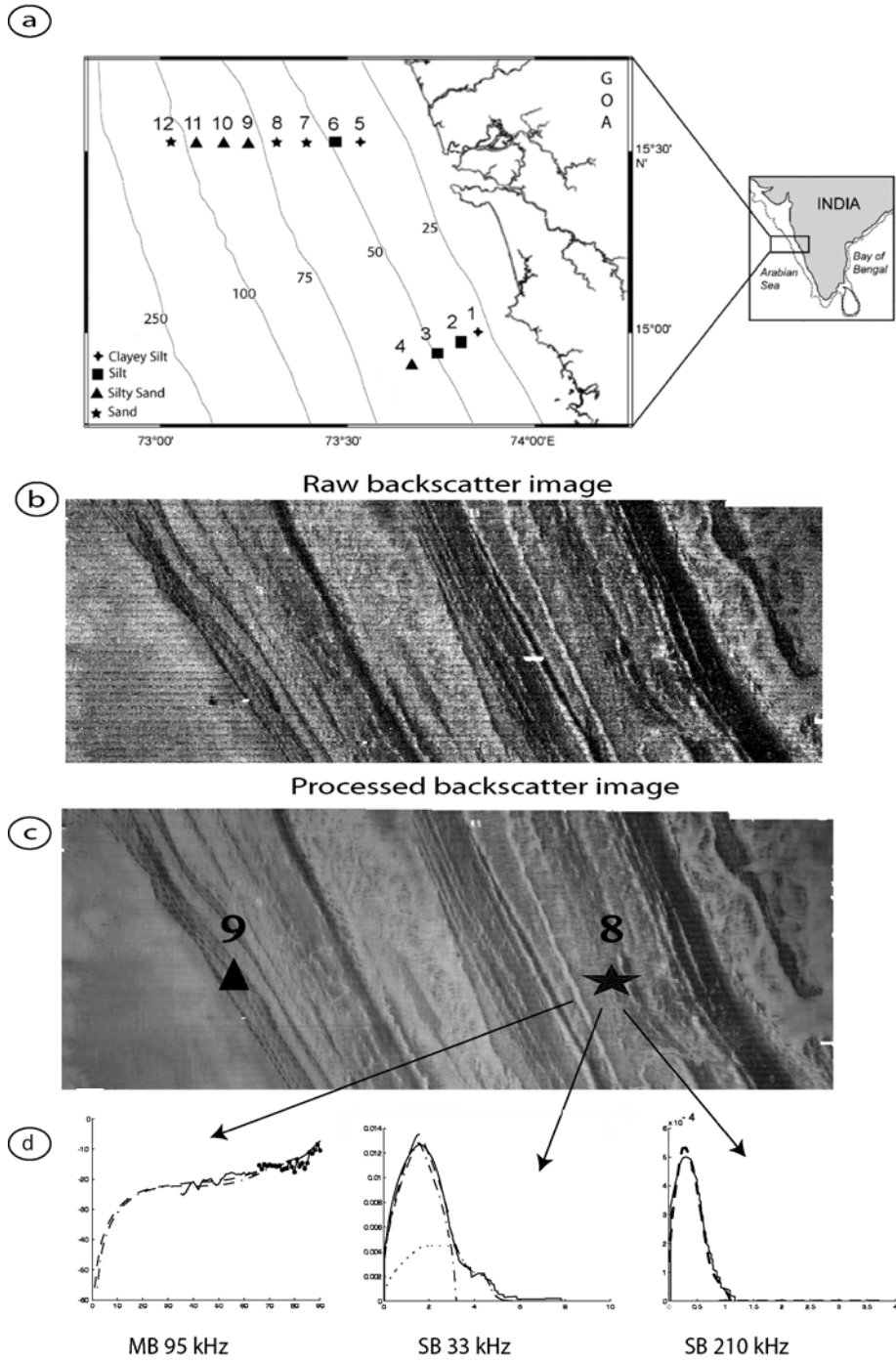


FIG. 1.

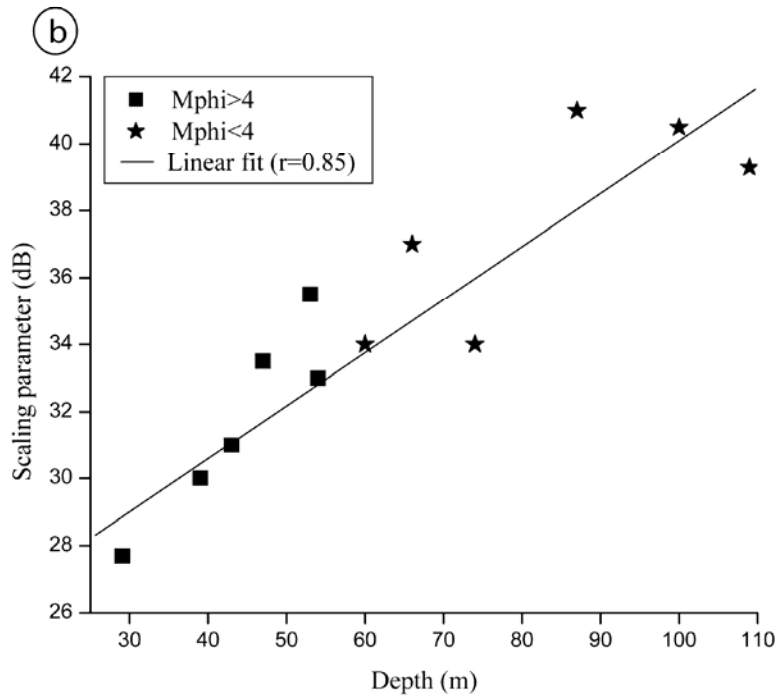
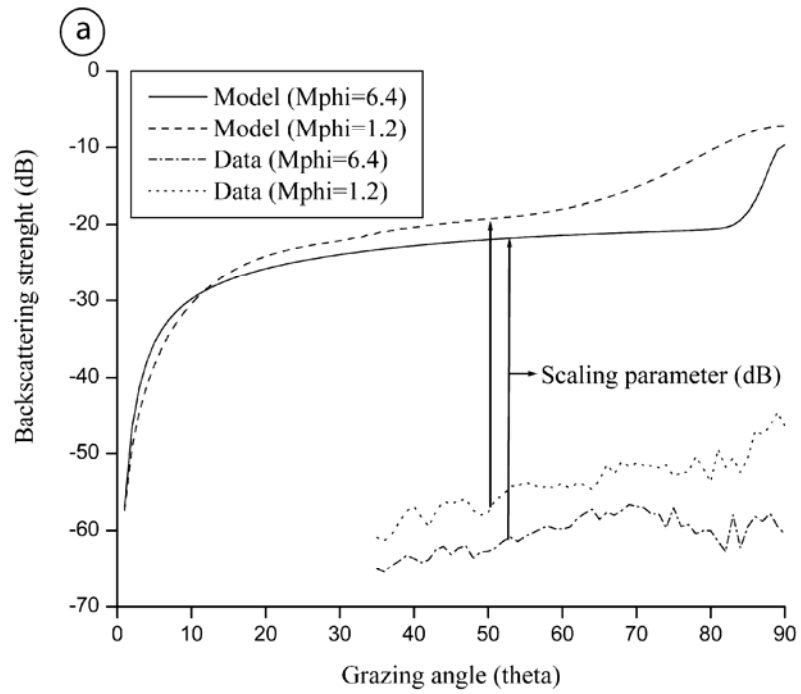


FIG. 2.

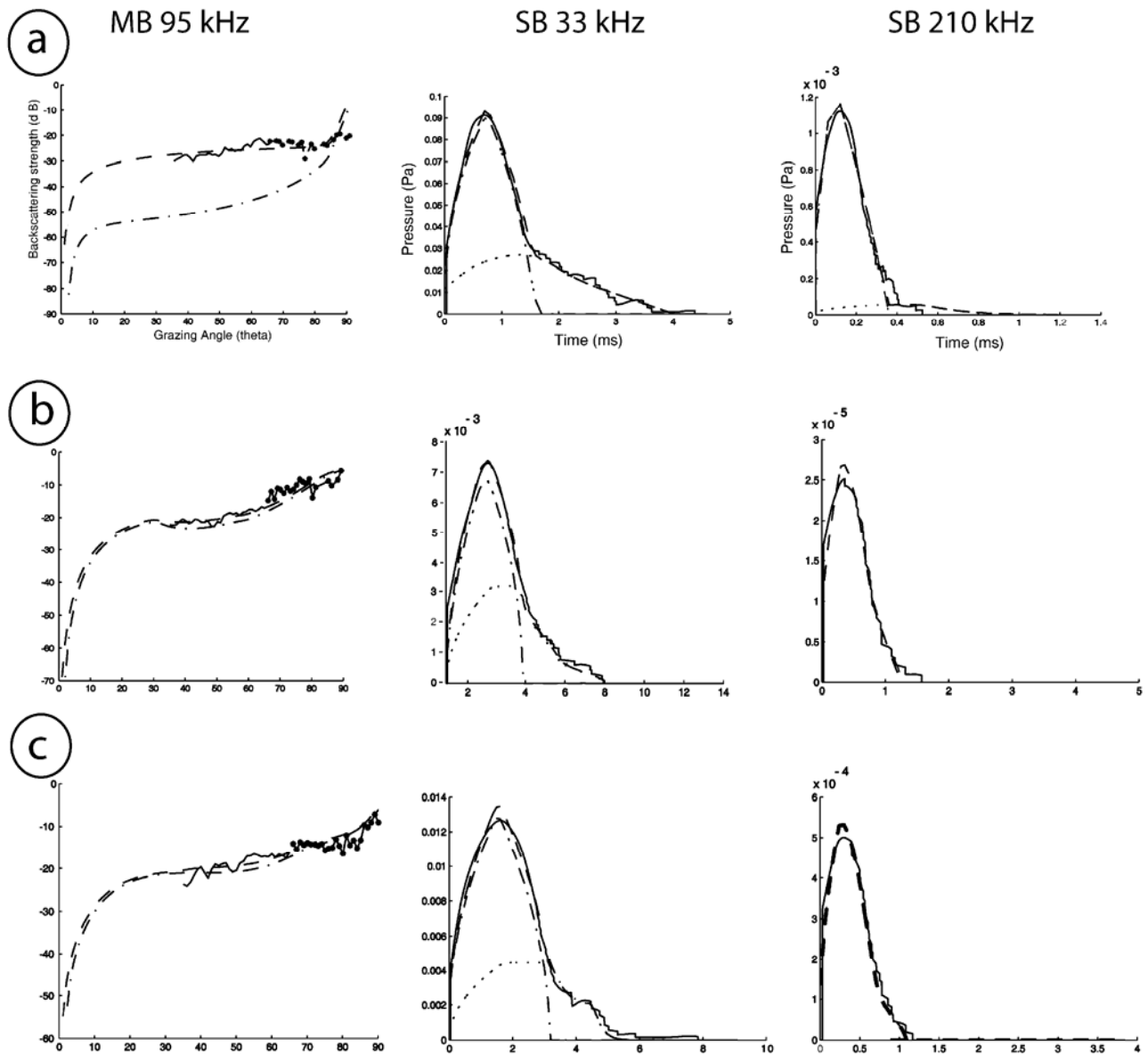


FIG. 3.

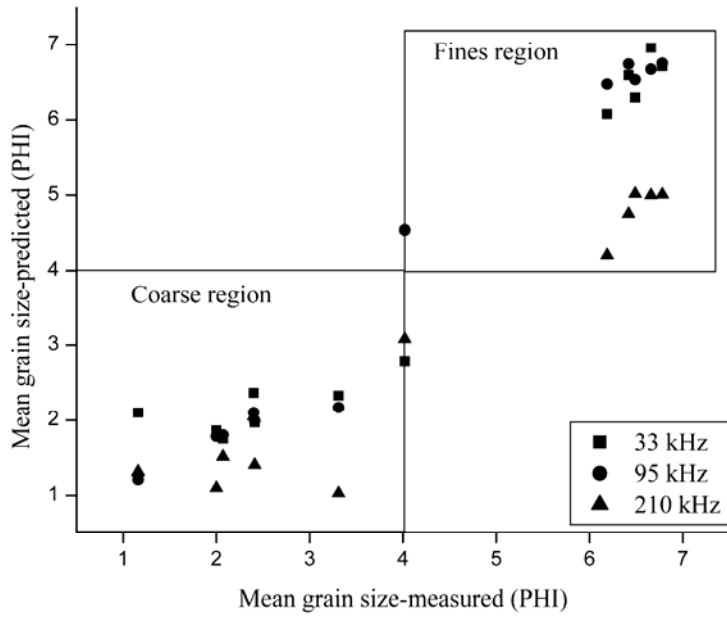


FIG. 4.

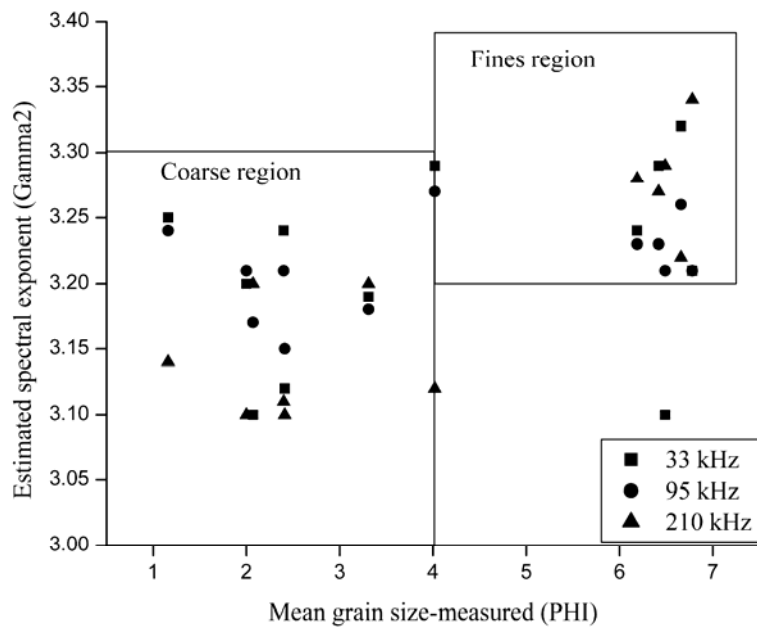


FIG. 5.

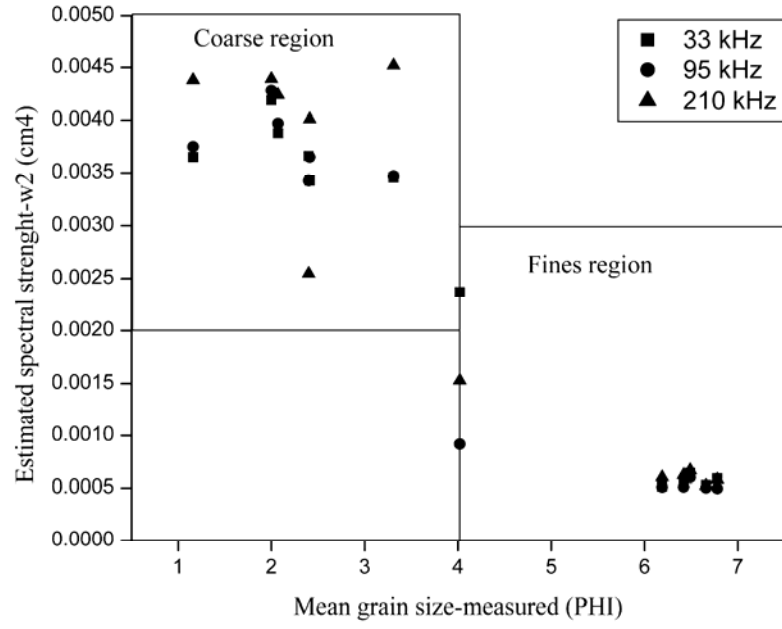


FIG. 6.

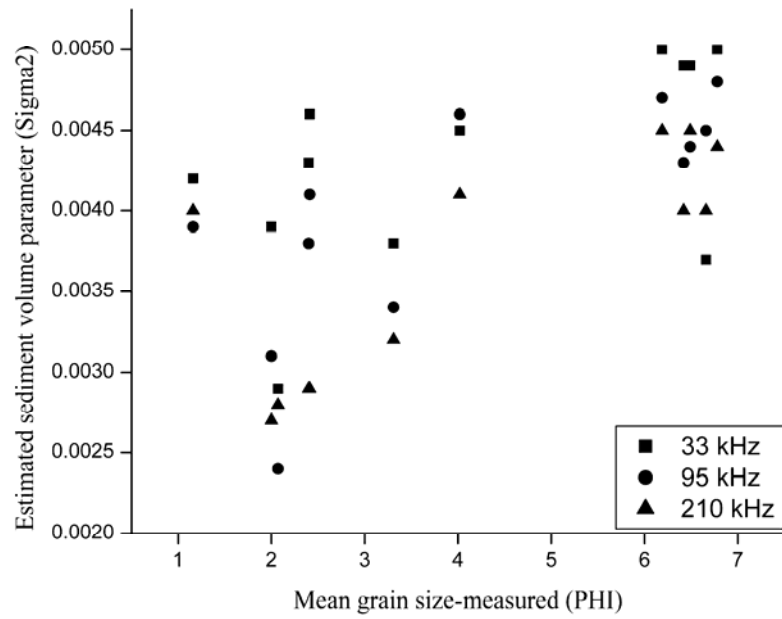


FIG. 7.